Article
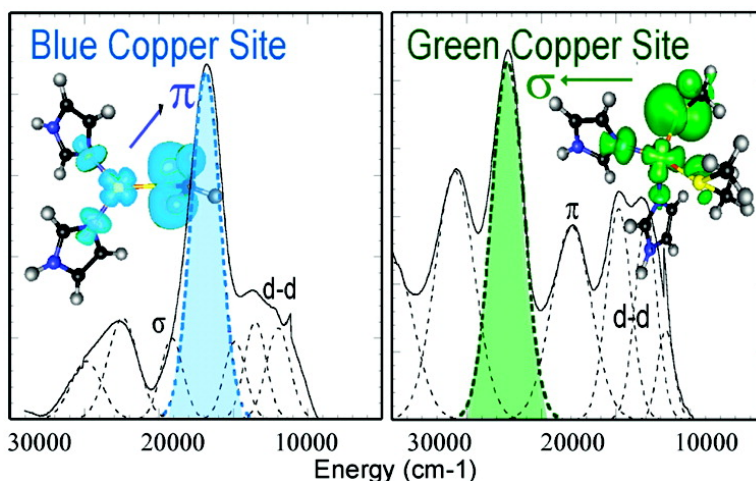
Spectroscopic Studies of the Met182Thr Mutant of Nitrite Reductase: Role of the Axial Ligand in the Geometric and Electronic Structure of Blue and Green Copper Sites

Lipika Basumallick, Robert K. Szilagyi, Yiwei Zhao, James P. Shapleigh, Charles P. Scholes, and Edward I. Solomon

More About This Article

Additional resources and features associated with this article are available within the HTML version:

- Supporting Information
- Links to the 8 articles that cite this article, as of the time of this article download
- Access to high resolution figures
- Links to articles and content related to this article
- Copyright permission to reproduce figures and/or text from this article

View the Full Text HTML

Spectroscopic Studies of the Met182Thr Mutant of Nitrite Reductase: Role of the Axial Ligand in the Geometric and Electronic Structure of Blue and Green Copper Sites

Lipika Basumallick,[†] Robert K. Szilagyi,[†] Yiwei Zhao,[‡,§] James P. Shapleigh,[⊥]
Charles P. Scholes,*[,‡] and Edward I. Solomon*[,†]

*Contribution from the Department of Chemistry, Stanford University,
Stanford, California, 94305, Department of Chemistry, Center for Biophysics and Biochemistry,
University at Albany, SUNY, Albany, New York 12222, and Department of Microbiology,
Wing Hall, Cornell University, Ithaca, New York 14853*

Received July 11, 2003; E-mail: edward.solomon@stanford.edu; cps14@albany.edu

Abstract: A combination of spectroscopic methods and density functional calculations has been used to describe the electronic structure of the axial mutant (Met182Thr) of *Rhodobacter sphaeroides* nitrite reductase in which the axial methionine has been changed to a threonine. This mutation results in a dramatic change in the geometric and electronic structure of the copper site. The electronic absorption data imply that the type 1 site in the mutant is like a typical blue copper site in contrast to the wild-type site, which is green. Similar ligand field strength in the mutant and the wild type (from MCD spectra) explains the similar EPR parameters for very different electronic structures. Resonance Raman shows that the Cu−S(Cys) bond is stronger in the mutant relative to the wild type. From a combination of absorption, CD, MCD, and EPR data, the loss of the strong axial thioether (present in the wild-type site) results in an increase of the equatorial thiolate−Cu interaction and the site becomes less tetragonal. Spectroscopically calibrated density functional calculations were used to provide additional insight into the role of the axial ligand. The calculations reproduce well the experimental ground-state bonding and the changes in going from a green to a blue site along this coupled distortion coordinate. Geometry optimizations at the weak and strong axial ligand limits show that the bonding of the axial thioether is the key factor in determining the structure of the ground state. A comparison of plastocyanin (blue), wild-type nitrite reductase (green), and the Met182Thr mutant (blue) sites enables evaluation of the role of the axial ligand in the geometric and electronic structure of type 1 copper sites, which can affect the electron-transfer properties of these sites.

1. Introduction

Blue copper proteins play a key role in long-range inter- and intraprotein electron transfer.[1−6] They are characterized by high reduction potentials, rapid electron-transfer rates, and unique spectral features compared to normal tetragonal copper complexes.[2,7] The classic blue site, such as plastocyanin, has a copper ion in a trigonally distorted tetrahedral environment. The trigonal plane has a very short (2.1 Å) Cu−S(Cys) and two typical (2.0

Å) Cu−N(His) ligands. The axial ligand is usually a S(Met) with a long Cu−S(Met) bond (2.8 Å).[8,9] These structural features impart the unique spectral features to the oxidized blue copper center, an intense ($\epsilon \approx 3000-6000$ M^{-1} cm^{-1}) absorption band near 600 nm, responsible for the "blue" color, and a small copper parallel hyperfine constant ($A_{\parallel} < 80 \times 10^{-4}$ cm^{-1}), which is reduced by more than a factor of 2 from normal Cu(II) centers. These characteristic spectral features are due to a very covalent (38%) Cu−S(Cys) bond, which facilitates rapid electron transfer over long distances (>13 Å).[10−14]

A number of perturbed sites within the family of blue copper proteins have also been investigated.[6,15−19] The perturbed blue copper site in nitrite reductase (enzyme involved in the catalysis

* To whom correspondence should be addressed.
† Stanford University.
‡ University at Albany.
⊥ Cornell University.
§ Present address: Wadsworth Center, NY State Department of Health, Empire State Plaza, P.O. Box 509, Albany, NY 12201-0509.

(1) Solomon, E. I.; Randall, D. W.; Glaser, T. *Coord. Chem. Rev.* **2000**, *200−202*, 595−632.
(2) Randall, D. W.; Gamelin, D. R.; LaCroix, L. B.; Solomon, E. I. *J. Biol. Inorg. Chem.* **2000**, *5*, 16−29.
(3) Adman, E. T. In *Advances in Protein Chemistry*; Anfinsen, C. B., Richards, F. M., Edsall, J. T., Eisenberg, D. S., Eds.; Academic Press: San Diego, 1991; Vol. 42, pp 145−198.
(4) Gray, H. B.; Solomon, E. I. *In Copper Proteins*; Wiley: New York, 1981.
(5) Solomon, E. I.; Lowery, M. D.; Guckert, J. A.; LaCroix, L. B. *Adv. Chem. Ser.* **1997**, *253*, 317−330.
(6) Solomon, E. I.; Baldwin, M. J.; Lowery, M. D. *Chem. Rev.* **1992**, *92*, 521−542.
(7) Messerschmidt, A. *Struct. Bond.* **1998**, *90*, 37−68.

(8) Colman, P. M.; Freeman, H. C.; Guss, J. M.; Murata, M.; Norris, V. A.; Ramshaw, J. A. M.; Venkatappa, M. P. *Nature* **1978**, *272*, 319−324.
(9) Guss, J. M.; Bartunik, H. D.; Freeman, H. C. *Acta Crystallogr.* **1992**, *B48*, 790−811.
(10) Lowery, M. D.; Guckert, J. A.; Gebhard, M. S.; Solomon, E. I. *J. Am. Chem. Soc.* **1993**, *115*, 5.
(11) Solomon, E. I.; Penfield, K. W.; Gewirth, A. A.; Lowery, M. D.; Shadle, S. E.; Guckert, J. A.; LaCroix, L. B. *Inorg. Chim. Acta* **1996**, *243*, 67−78.
(12) Crane, B. R.; DiBilio, A. J.; Winkler, J. R.; Gray, H. B. *J. Am. Chem. Soc.* **2001**, *123*, 11623−11631.
(13) Daizadeh, I.; Medvedev, E. S.; Stuchebrukhov, A. A. *Prod. Natl. Acad. Sci. U. S. A.* **1997**, *94*, 3703−3708.
(14) Farver, O.; Pecht, I. *Adv. Chem. Phys.* **1999**, *107*, 555−589.

of the reduction of nitrite to nitric oxide, $NO_2^- + 2H^+ + e^- \rightarrow NO + H_2O$ a key step in the denitrifying pathway of anaerobic bacteria) has the same ligand set as plastocyanin. However, the changes in the spectral features (decreased 600 nm band intensity and increased absorption intensity at 450 nm, leading to its green color) indicate that the Cu−S(Cys) interaction in the highest occupied molecular orbital (HOMO) is rotated from a pure π (in the typical blue copper site of plastocyanin) to a σ bonding interaction.[18] The magnetic circular dichroism (MCD) spectra show that the ligand field transitions shift to higher energy in nitrite reductase. This reflects a tetragonal distortion of the ligand field in going from plastocyanin to nitrite reductase. The effective stretching frequency of the Cu−S(Cys) bond (from resonance Raman) decreases in nitrite reductase (relative to plastocyanin), indicating a weakened thiolate Cu−S(Cys) bond. The crystal structure of the active site in nitrite reductase revealed that the axial Cu−S(Met) bond length decreases (2.6 Å) and the equatorial Cu−S(Cys) bond length increases (2.17 Å) compared to plastocyanin.[20] This has led to the formulation of the *coupled distortion* model[18] for the perturbed site of nitrite reductase in which the axial Cu−S(Met) interaction strengthens, the equatorial Cu−S(Cys) bond weakens, and the S(Cys)−Cu−S(Met) plane rotates relative to the N(His)−Cu−H(His) plane toward a more tetragonal geometry at the copper center. The major change in the electronic structure is the rotation of the Cu $3d_{x^2−y^2}$ HOMO about the Cu−S(Met) bond. This rotation along with the tetragonal distortion allows for significant σ interaction of the S(Cys) with the Cu half-occupied HOMO. The electronic and geometric differences between the perturbed blue site in nitrite reductase and the classical blue site in plastocyanin can contribute to differences in the electron-transfer properties of these sites.[1] Further, it is interesting to note that there are copper-containing reductases (e.g., *Alcaligenes xylosoxidans* nitrite reductase[21,22]) which are blue. However, they do not exhibit the tetragonal distortion (the $N_{His}CuN_{His}$ to $S_{Cys}CuS_{Met}$ dihedral angle (φ) is 75° vs 62° in the green nitrite reductase) and are spectroscopically similar to typical blue copper sites.

The studies on the electronic and geometric structure of classical and perturbed blue copper sites have been extended to the axial mutant of nitrite reductase (Met182Thr) where the axial methionine residue has been mutated to a threonine.[23] This in principle replaces this shorter, stronger S(Met) of wild-type nitrite reductase with no axial ligand. This mutation results in an intense absorption at 600 nm and weaker absorption intensity at 450 nm, more typical absorption features of classical blue

copper sites. However, the Met182Thr oxidized ground-state properties (*g* values, copper hyperfine values, and ENDOR frequencies) were unchanged from their values in the wild-type enzyme.[24]

In this present study, the electronic structure of the mutant has been defined relative to the wild-type nitrite reductase and to the classical blue sites of plastocyanin and fungal laccase[25] (a blue site with no axial ligation) in order to understand the influence of the axial ligand on the geometric and electronic structure of the site. Spectroscopic techniques including low-temperature absorption, magnetic circular dichroism, circular dichroism, and resonance Raman have been complemented by spectroscopically calibrated density functional calculations to probe the electronic structure of the Met182Thr mutant of nitrite reductase. In conjunction with experiments, the calculations generate a detailed description of bonding at the copper center in the mutant relative to the wild-type protein and its contribution to the properties of both sites. Geometric optimizations with and without the axial S(Met) evaluate the role of the axial ligand in determining the geometric and electronic structure of blue and green copper sites.

2. Experimental Section

2.1. Samples. Wild-type and the Met182Thr mutant forms of *Rhodobacter sphaeroides* nitrite reductase were prepared by overexpression in *Escherichia coli* as described elsewhere.[23] To make type 2 depleted (T2D) samples, the enzyme was dialyzed at 4 °C vs nitrogen-flushed 50 mM pH 6.2 phosphate buffer that contained 2 mM dimethylglyoxime, 1 mM EDTA, and 5 mM ferrocyanide. For T2D depletion of the wild-type protein, the copper-removing dialysis took about 6 h; for longer dialysis a color loss was noted that indicated undesirable loss of the type 1 site. For T2D depletion of the Met182Thr mutant we allowed the copper-removing dialysis treatment to last for only 3 h, because loss of type 1 copper (and precipitation of protein) occurred with longer treatment. The shorter copper-removing dialysis for the T2D derivative of the Met182Thr mutant allowed 40% of the type 2 copper to remain, based on EPR spin quantitation. Spin quantitation was accomplished by using a copper standard, $Cu(ClO_4)_2$,[26] of known concentration run in the same tube as the sample. Protein samples ($\sim 0.5−1.0$ mM, concentrated using Amicon or Microcon concentrators) were prepared as glasses in 50% (v/v) D_2O/glycerol-d_3 in 100 mM phosphate (pD* = 6.8). Samples were transferred to quartz EPR tubes and MCD cells for spectroscopic characterization. Addition of glycerol had no effect on the CD of the proteins. Chemicals used as buffers were reagent grade and were used without further purification. Water was purified to resistivity of $15−18$ MΩ with a Barnstead Nanopure deionizing system.

2.2. UV−Vis Electronic Absorption and Circular and Magnetic Circular Dichoism. Absorption spectra at temperatures between 5 and 300 K were obtained using a computer-interfaced Cary-500 spectrophotometer modified to accommodate a Janis Research Super Vari-Temp cryogenic Dewar mounted in the light path. Low-temperature circular dichroism and magnetic circular dichroism were performed using two Jasco spectropolarimeters. Each is equipped with a modified sample compartment to accommodate focusing optics and an Oxford Instruments SM4000-7T superconducting magnet/cryostat. This arrangement allows data collection at temperatures from 1.6 to 290 K and fields up to 7 T.[27] A Jasco J810 spectropolarimeter operating with

(15) Adman, E. T. *Topics in Molecular and Structural Biology: Metalloproteins*; Macmillan: New York, 1985; Vol. 1.

(16) Gewirth, A. A.; Cohen, S. L.; Schugar, H. J.; Solomon, E. I. *Inorg. Chem.* **1987**, *26*, 1133−1146.

(17) Lu, Y.; LaCroix, L. B.; Lowery, M. D.; Solomon, E. I.; Bender, C. J.; Peisach, J.; Roe, J. A.; Gralla, E. B.; Valentine, J. S. *J. Am. Chem. Soc.* **1993**, *115*, 5907−5918.

(18) LaCroix, L. B.; Shadle, S. E.; Wang, Y. N.; Averill, B. A.; Hedman, B.; Hodgson, K. O.; Solomon, E. I. *J. Am. Chem. Soc.* **1996**, *118*, 7755−7768.

(19) LaCroix, L. B.; Randall, D. W.; Nersissian, A. M.; Hoitink, C. W. G.; Canters, G. W.; Valentine, J. S.; Solomon, E. I. *J. Am. Chem. Soc.* **1998**, *120*, 9621.

(20) Adman, E. T.; Godden, J. W.; Turley, S. *J. Biol. Chem.* **1995**, *270*, 27458−27474.

(21) Dodd, F. E.; Beeumen, V.; Eady, R. R.; Hasnain, S. S. *J. Mol. Biol.* **1998**, *282*, 369−382.

(22) Ellis, M. J.; Dodd, F. E.; Sawers, G.; Eady, R. R.; Hasnian, S. S. *J. Mol. Biol.* **2003**, *328*, 429−438.

(23) Olesen, K.; Veselov, A.; Zhao, Y.; Wang, Y.; Danner, B.; Scholes, C. P.; Shapleigh, J. P. *Biochemistry* **1998**, *37*, 6086−6094.
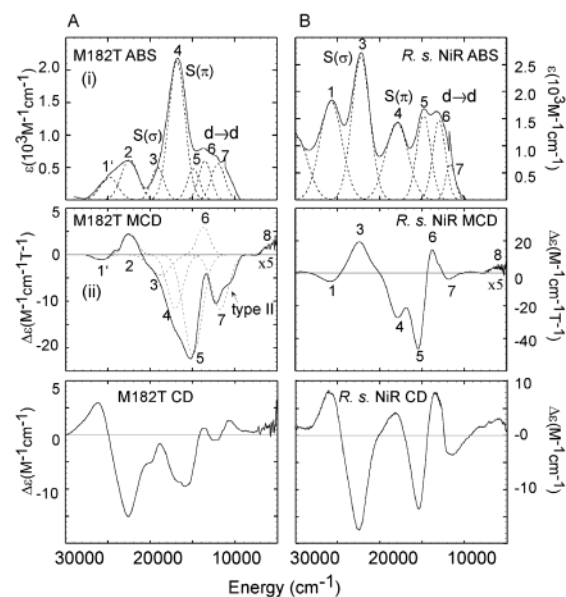
(24) Veselov, A.; Olesen, K.; Seinkiewicz, A.; Shapleigh, J. P.; Scholes, C. P. *Biochemistry* **1998**, *37*, 6095−6105.

(25) Palmer, A. E.; Randall, D. W. R.; Xu, F.; Solomon, E. I. *J. Am. Chem. Soc.* **1999**, *121*, 7138−7149.

(26) Carithers, R. P.; Palmer, G. *J. Biol. Chem.* **1981**, *256*, 7967−7976.

(27) Allendorf, M. D.; Spira, D. J.; Solomon, E. I. *Prod. Natl. Acad. Sci. U. S. A.* **1985**, *82*, 3063−3067.

a S-20 photomultiplier tube was used to access the visible and ultraviolet spectral region. A Jasco J200 spectropolarimeter operating with a liquid nitrogen cooled InSb detector was used for the near-infrared region. Special care was taken to provide magnetic shielding for the PMT detector. Depolarization of the light by the MCD samples was monitored by their effect on the CD signal of nickel (+)-tartarate placed before and after the sample. In all cases the depolarization was less than 5%.[28] CD samples were run in a 1.0-cm quartz cuvette. MCD samples were run in MCD cells fitted with quartz disks and a 0.3-cm rubber gasket spacer. Simultaneous Gaussian fitting of the absorption, MCD, and CD spectra was performed with the Peak-Fit program (Jandel).

2.3. Resonance Raman. Resonance Raman spectra were collected with a Princeton Instruments ST-135 back-illuminated CCD detector on a Spex 1877 CP triple monochromator with 1200, 1800, and 2400 grooves/mm holographic spectrograph gratings. Continuous wave coherent Kr ion (Innova90C-K) and an Ar ion (Sabre-25/7) visible and UV laser lines were used as variable excitation sources. A polarization scrambler was used between the sample and the spectrometer. The Raman energy was calibrated with Na_2SO_4. Frequencies are accurate to within <2 cm^{-1}. Samples were loaded in 4-mm NMR tubes and stored in liquid nitrogen.

2.4. Electronic Structure Calculations. Gradient-corrected density functional calculations (GGA-DFT) were carried out by using a Gaussian98[29] package on a 80-cpu heterogeneous cluster of SGI and IBM PC compatible computers. The Becke88[30] exchange and Perdew86[31] correlation nonlocal functionals were used with Wosko-Vilk-Nussair local functionals[32] as implemented in the software package (BP86). The triple-ζ (VTZ*)[33] and double-ζ (6-31G*)[34−36] Gaussian type all-electron basis sets (BS5) were employed with polarization functions for the metal and ligand atoms, respectively. These basis sets have been previously shown to be theoretically converged for Cu^{II}-containing systems and additional polarization or diffuse functions do not improve the electronic structure description.[37−39] Since the standard GGA-DFT calculations give too much ligand character in the ground-state wave function compared to experiment, 38% of total DF exchange was replaced with HF exchange (B(38HF)P86), giving an accurate bonding description as discussed for other cupric systems.[39] Population analyses were performed by means of Weinhold's natural population analysis[40−42] (NPA), including the Cu 4p orbitals in the valence set.

The computational models of the active sites were constructed from imidazole, methyl thiolate, and dimethyl thioether molecules. The

(28) Browett, W. R.; Fucaloro, A. F.; Morgan, T. V.; Stephens, P. J. *J. Am. Chem. Soc.* **1983**, *105*, 1868−1872.
(29) Frisch, M. J.; Trucks, G. W.; Schlegel, H. B.; Scuseria, G. E.; Robb, M. A.; Cheeseman, J. R.; Zakrzewski, V. G.; Montgomery, J. A. J.; Stratmann, R. E.; Burant, J. C.; Dapprich, S.; Millam, J. M.; Daniels, A. D.; Kudin, K. N.; Strain, M. C.; Farkas, O.; Tomasi, J.; Barone, V.; Cossi, M.; Cammi, R.; Mennucci, B.; Pomelli, C.; Adamo, C.; Clifford, S.; Ochterski, J.; Petersson, G. A.; Ayala, P. Y.; Cui, Q.; Morokuma, K.; Malick, D. K.; Rabuck, A. D.; Raghavachari, K.; Foresman, J. B.; Cioslowski, J.; Ortiz, J. V.; Stefanov, B. B.; Liu, G.; Liashenko, A.; Piskorz, P.; Komaromi, I.; Gomperts, R.; Martin, R. L.; Fox, D. J.; Keith, T.; Al-Laham, M. A.; Peng, C. Y.; Nanayakkara, A.; Gonzalez, C.; Challacombe, M.; Gill, P. M. W.; Johnson, B.; Chen, W.; Wong, M. W.; Andres, J. L.; Head-Gordon, M.; Replogle, E. S.; Pople, J. A.; Revision A.1 ed. ed.; Gaussian, Inc.: Pittsburgh, PA, 1998.
(30) Becke, A. D. *Phys. Rev. A* **1988**, *38*, 3098−3100.
(31) Perdew, J. P. *Phys. Rev. B* **1986**, *33*, 8822−8824.
(32) Vosko, S. H.; Wilk, L.; Nusair, M. *Can. J. Phys.* **1980**, *58*, 1200−1211.
(33) Schaefer, J.; Horn, H.; Ahlrichs, R. *J. Chem. Phys.* **1992**, *97*, 2571−2577.
(34) Hariharan, P. C.; Pople, J. A. *Theor. Chim. Acta* **1973**, *28*, 213−222.
(35) Francl, M. M.; Hehre, W. J.; Binkley, J. S.; Gordon, M. S.; DeFrees, D. J.; Pople, J. A. *J. Chem. Phys.* **1982**, *77*, 3645−3665.
(36) Rassolov, V. A.; Pople, J. A.; Ratner, M. A.; Windus, T. L. *J. Chem. Phys.* **1998**, *109*, 1223−1229.
(37) Siegbahn, P. E.; Blomberg, M. R. A. *Chem. Rev.* **2000**, *100*, 421−437.
(38) Ryde, U.; Olsson, M. H. M.; Pierloot, K. *Theor. Comput. Chem.* **2001**, *9*, 1−55.
(39) Szilagyi, R. K.; Metz, M.; Solomon, E. I. *J. Chem. Phys.* **2002**, *106*, 2994−3007.
(40) Foster, J. P.; Weinhold, F. *J. Am. Chem. Soc.* **1980**, *102*, 7211−7218.
(41) Reed, A. E.; Curtiss, L. A.; Weinhold, F. *Chem. Rev.* **1988**, *88*, 8, 899−926.
(42) Carpenter, J. E.; Weinhold, F. *THEOCHEM* **1988**, *169*, 41−62.

Figure 1. Electronic absorption (top), magnetic circular dichroism (middle), and circular dichroism (bottom) spectra of Met182Thr mutant (A) and wild type of *Rhodobacter sphaeroides* nitrite reductase (B). The derivative-shaped MCD feature at 24 000 cm^{-1} (* in Figure 1A ii) in the M182T mutant is due to a small amount of heme present in the protein sample. Band 2 is not labeled in the wild-type nitrite reductase spectra because it cannot be resolved due to overlap with bands 1 and 3.

atomic coordinates of the blue Cu (1PLC, 1.33 Å res.), green Cu (1NIA, 2.50 Å res.) and fungal laccase (1A65, 2.23 Å res.) active site geometries were taken from the X-ray structures of the poplar plastocyanin (*Populus nigra*),[9] nitrite reductase from *Achromobacter cycloclastes*,[43] and laccase from *Coprinus cinereus*,[44] respectively.

Geometry optimizations were performed with frequent updates of the force constants in order to stay as close as possible to the lowest energy pathway. Stationary points were restarted with continuous update of force constants until the optimization terminated due to negligible forces. In all optimizations, the GDIIS[45−47] optimizer was applied due to the flat potential energy surface of the Cu site.

3. Results and Analysis.

3.1. Absorption, Circular Dichroism, and Magnetic Circular Dichroism. Spectroscopic properties of the wild type are compared to those of the type 2 depleted enzyme in the supplementary information (S1). This allows the study of the type 1 site and identifies the type 2 spectral features. The absorption and MCD spectra for the wild-type and the type 2 depleted enzymes are essentially the same, suggesting that the removal of the type 2 copper does not affect the type 1 site. Detailed comparison (in S1B inset) reveals a small MCD feature, which is attributed to the type 2 copper. Low-temperature absorption, CD, and MCD spectra in the region from 5000 to 30000 cm^{-1} for the type 2 depleted (containing 40% type 2, see Section 2.1) Met182Thr mutant are presented in Figure 1A and for type 2 depleted wild-type nitrite reductase in Figure 1B. Gaussian resolution of the absorption spectra for the Met182Thr mutant and the wild-type nitrite reductase obtained from a simultaneous

(43) Adman, E. T.; Godden, J. W.; Turley, S. *J. Biol. Chem.* **1995**, *270*, 27458−27474.
(44) Ducros, V.; Brzozowski, A. M.; Wilson, K. S.; Brown, S. H.; Ostergaard, P.; Schneider, P.; Yaver, D. S.; Pederson, A. H.; Davies, G. J. *Nature Struct. Biol.* **1998**, *5*, 310−316.
(45) Csaszar, P.; Pulay, P. *J. Mol. Struct. (THEOCHEM)* **1984**, *114*, 31−34.
(46) Farkas, O.; Schlegel, H. B. *J. Chem. Phys.* **1998**, *109*, 7100−7104.
(47) Farkas, O.; Schlegel, H. B. *J. Chem. Phys.* **1999**, *111*, 10806−10814.

Table 1. Experimental Spectroscopic Parameters for *Rhodobacter sphaeroides* Nitrite Reductase Met182Thr Mutant

band	energy, cm^{-1}	ϵ, M^{-1}cm^{-1}	$\Delta\epsilon$, M^{-1}cm^{-1}T^{-1}	C_0/D_0
8	5 800		+^{a}	+^{a}
7	12 000	630	−11.8	−0.14
6	13 500	760	+6.5	+0.10
5	14 800	620	−22.0	−0.26
4	16 800	2170	−11.6	−0.04
3	19 100	630	−4.0	−0.04

^{a} Only signs can be determined from the data for these parameters; however, the C_0/D_0 ratio should be greater than 0.1 on the basis of the relative magnitude of MCD to upper ϵ limit in absorption.

fit of the absorption, CD, and MCD spectra for each protein are included in the top panels of Figure 1. Energies and ϵ (M^{-1} cm^{-1}) values for the absorption bands determined from these fits are summarized in Table 1. To be consistent with other blue copper proteins, we have used the numbering scheme from plastocyanin.[48,49]

3.1.1. Band Assignments. Bands observed in the absorption and MCD spectra can be classified as ligand field or charge transfer by comparing their relative intensities in MCD and absorption. This parameter is the ratio of C_0, the MCD *C*-term intensity, and D_0, the dipole strength in absorption. C_0/D_0 ratios were determined from the Gaussian fit of the MCD taken within the linear $1/T$ region and the absorption spectra[50] by using the relation

$$C_0/D_0 = (kT\Delta\epsilon)/(\mu_B B\epsilon_{max})$$

where T is the temperature, B is the external magnetic field strength, k is the Boltzmann's constant, μ_B is the Bohr magneton, ϵ_{max} is the absorption maximum in M^{-1} cm^{-1}, and $\Delta\epsilon$ is the MCD intensity maximum measured in M^{-1} cm^{-1} ($k/\mu_B \approx 1.489$ TK^{-1}). MCD intensity depends on the spin−orbit coupling for the center involved in the transition. The spin−orbit coupling for Cu is greater than for S or N (ξ(Cu) = 830 cm^{-1}, ξ(S) = 382 cm^{-1}, and ξ(N) = 70 cm^{-1}). Therefore, transitions centered on Cu (i.e., d → d) have a higher *C*-term MCD intensity than charge-transfer transitions that involve significant S or N character. Alternatively, ligand−ligand overlap determines the absorption intensity and is greater for the two levels involved in a charge-transfer transition. Specific assignments for the transitions were made on the basis of the magnitude and sign of C_0/D_0 relative to plastocyanin.

In the low-energy region (<16 000 cm^{-1}) five bands are observed at 5800 cm^{-1} (band 8), 10 000 cm^{-1} (labeled as type 2 in Figure 1A (ii); to be discussed below), 12 000 cm^{-1} (band 7), 13 500 cm^{-1} (band 6), and 14 800 cm^{-1} (band 5), in the Met182Thr mutant. Four higher energy bands in the Met182Thr mutant are observed at 16 800 cm^{-1} (band 4), 19 100 cm^{-1} (band 3), 22 500 cm^{-1} (band 2), and 25 000 cm^{-1} (band 1′). The highest energy band has been labeled 1′ because it has a different spectral pattern and a different assignment from band 1 of plastocyanin (vide infra). The wild-type nitrite reductase spectrum is characterized by four bands in the low energy region at 5600 cm^{-1} (band 8), 11900 cm^{-1} (band 7), 13500 cm^{-1} (band

(48) Penfield, K. W.; Gay, R. R.; Himmelwright, R. S.; Eickman, N. C.; Freeman, H. C.; Solomon, E. I. *J. Am. Chem. Soc.* **1981**, *103*, 4382−4388.
(49) Gewirth, A. A.; Solomon, E. I. *J. Am. Chem. Soc.* **1988**, *110*, 3811−3819.
(50) Piepho, S. B.; Schatz, P. N. In *Group Theory in Spectroscopy: With Applications to Magnetic Circular Dichroism*; John Wiley & Sons: New York, 1983.

6) and 14900 cm^{-1} (band 5) and three bands at 17550 cm^{-1} (band 4), 21900 cm^{-1} (band 3) and 25650 cm^{-1} (band 1) in the higher energy region. (A counterpart for band 2 in plastocyanin cannot be resolved from the spectra of wild-type nitrite reductase, due to overlap with bands 1 and 3.)

The five lower energy bands (bands 5−8, see Table 1) in the Met182Thr mutant are assigned as ligand field transitions as they exhibit $|C_0/D_0| \sim 0.10$. On the basis of the MCD sign and intensity of band 5 (14 800 cm^{-1}) as compared to that of plastocyanin, this band is assigned to the d$_{xz}$ → d$_{x^2-y^2}$ transition. This band is usually the most intense negative feature in the MCD spectrum of blue copper proteins.[18,19,49] Band 6 (13 500 cm^{-1}) is not resolved in the MCD spectrum. However, it is clearly present in the CD spectrum and is required by the simultaneous fit of the absorption, CD, and MCD. It is not resolved in the MCD because it overlaps with the two negative features due to band 5 (14 800 cm^{-1}) and band 7 (12 000 cm^{-1}), which are closer in energy by ∼200 cm^{-1} in the Met182Thr mutant relative to wild-type nitrite reductase. Band 6 (13 500 cm^{-1}) is attributed to the d$_{xz+yz}$ → d$_{x^2-y^2}$ transition based on its positive sign in MCD as is typically observed for blue copper sites. Band 7 (12 000 cm^{-1}) is assigned to the d$_{xy-yz}$ → d$_{x^2-y^2}$ transition. The lowest energy band (band 8, 5800 cm^{-1}) is present in the MCD and CD spectra. This ligand field band is assigned to the d$_{z^2}$ → d$_{x^2-y^2}$ transition.

The Met182Thr mutant shows an additional band at ∼10 000 cm^{-1} in the CD and the MCD (shoulder at 10 000 cm^{-1}) spectra compared to typical blue copper spectra. To assign the 10 000 cm^{-1} band, the spectroscopic properties of the wild-type nitrite reductase were compared to those of the type 2 depleted wild-type enzyme (supplement information; Figure S1). This allowed the identification of the spectral features of the type 2 site. This revealed the presence of a band at ∼10 000 cm^{-1} only in the holoenzyme, which is thus assigned as a type 2 copper ligand field transition. It is observable because it occurs in a spectroscopically silent portion of the blue copper MCD spectrum. Analogously, the band at 10 000 cm^{-1} in the MCD spectrum of the Met182Thr mutant is assigned as a type 2 copper ligand field transition. The presence of this band in the "type 2 depleted" spectrum of Met182Thr results from incomplete removal of the type 2 sites. EPR data (supplement information; Figure S2) confirm the presence of some residual type 2 copper (∼40%) in the type 2 depleted Met182Thr mutant sample.

In the Met182Thr mutant, band 4 at 16 800 cm^{-1} has very high absorption intensity (ϵ_{max} = 2170 M^{-1} cm^{-1}) and relatively low MCD intensity ($|\Delta\epsilon|$ = 12 M^{-1} cm^{-1}) and is the intense absorption feature responsible for the blue color of this mutant. In analogy to other well-characterized blue copper proteins, this band involves the π Cu−S bonding interaction and is assigned as the S 3pπ → Cu 3d$_{x^2-y^2}$ charge-transfer transition.[18,19,49] Note that EPR ($g_{||} > g_\perp > 2.0023$)[23] and density functional calculations (vide infra) identify d$_{x^2-y^2}$ as the highest singly occupied molecular orbital (SOMO). At a higher energy the MCD spectrum of Met182Thr exhibits a relatively weak band at 19 100 cm^{-1} (band 3), which can be assigned to the S 3p pseudo σ → Cu 3d$_{x^2-y^2}$ charge-transfer transition, by analogy to plastocyanin. The higher energy bands at 22 500 cm^{-1} (band 2) and 25 000 cm^{-1} (band 1′) are assigned to charge-transfer transitions from the equatorial histidine ligands (vide infra).

Table 2. Experimental Spectroscopic Parameters for Spinach Plastocyanin, *Rhodobacter sphaeroides* Nitrite Reductase Met182Thr Mutant, *Rhizoctonia solani* Fungal Laccase, and *Rhodobacter sphaeroides* Nitrite Reductase[a]

band	energy, cm^{-1}	plastocyanin	Met182Thr	fungal laccase	WT NiR
8	d_{z^2}	5 000	5 800	6 500	5 600
7	d_{xy}	10 800	12 000	13 080	11 900
6	d_{xz+yz}	12 800	13 500	14 590	13 500
5	d_{xz-yz}	13 950	14800	15 850	14 900
4	Cys π	16 700	16 800	16 660	17 500
3	pseudo-σ	18 700	19 100	18 640	21 900

[a] Parameters for plastocyanin and fungal laccase were reported previously in refs 18 and 25. The energy for the d_{z^2} transition is taken from the low-temperature MCD, whereas the energies of the remainder transitions are taken from the low-temperature absorption.

3.1.2. Comparison with Plastocyanin and Fungal Laccase.
Comparison of the Met182Thr spectral features with those of plastocyanin[48,49] and fungal laccase[25] quantitates the nature of the blue copper center in the mutant. The blue copper center in plastocyanin is characterized by three equatorial ligands (two histidines and a cysteine) and a weak axial methionine ligand. The blue copper center in fungal laccase is tricoordinate and lacks the axial ligand. The charge-transfer region of Met182Thr is qualitatively similar to that in plastocyanin and fungal laccase, exhibiting the strong ~595 nm and weak ~450 nm absorption intensity pattern. In the Met182Thr mutant the d → d transition energies are between those of plastocyanin and fungal laccase (Table 2). The energies of d → d transitions are very sensitive to the ligand field at the copper center, which is determined by the extent of axial and equatorial ligand interactions. The increase in axial interaction on going from fungal laccase (no axial ligand) to plastocyanin (weak S(Met) axial ligand) results in the displacement of the metal out of the trigonal plane of the equatorial ligands toward the axial ligand by 0.33 Å. The net effect of this is to decrease the ligand field and thus the d → d transition energies on going from fungal laccase to plastocyanin. The d → d transition energies of Met182Thr (lower than fungal laccase but higher than in plastocyanin) reflect a ligand field strength for Met182Thr intermediate between those of plastocyanin and fungal laccase. The type 1 copper center in Met182Thr has a substantially weaker (but nonzero) axial interaction compared to plastocyanin, in addition to the two histidines and the cysteine equatorial ligands. Threonine, which has replaced the axial methionine in the mutant, could provide the relatively weak interaction or be replaced by water or by a protein endogenous ligand. Preliminary X-ray data[51] suggest that the last possibility can be eliminated.

This is also reflected in the change in the energy of the d_{z^2} → $d_{x^2-y^2}$ transition (band 8) in going from plastocyanin (5000 cm^{-1}) to Met182Thr (5800 cm^{-1}) and to fungal laccase (6500 cm^{-1}). The d_{z^2} transition energy increases as the strength of the axial ligand decreases, because d_{z^2} is antibonding with respect to the axial ligand.

The higher energy region (beyond the cysteine-based charge-transfer transitions) of plastocyanin is characterized by two charge-transfer transitions at 21 390 cm^{-1} (band 2) and 23 440 cm^{-1} (band 1) derived from the N(His)→Cu and S(Met)→Cu charge-transfer transitions. In the tricoordinate fungal laccase,[25] two transitions are observed in this region at ~22 500 and ~25 000 cm^{-1}. In yeast Fet3p[52] (also a three-coordinate type 1 blue copper center), the two high-energy transitions are at 22 400

and 26 500 cm^{-1}. The Met182Thr mutant also exhibits two transitions at 22 500 and 25 000 cm^{-1}.

In a detailed spectroscopic and electronic structure comparative study[53] of plastocyanin and the tris(pyrazolyl)hydroborate triphenylmethylthiolate Cu(II) model complex, it is clearly seen that the π_1 imidazole ligand based orbitals contribute to the absorption intensity for band 2 at 21 390 cm^{-1}. Q-band ^{14}N ENDOR studies have shown that the two histidine nitrogens are equivalent in plastocyanin ($A^{N1} \sim A^{N2} \sim$ 22 MHz), while they are inequivalent in fungal laccase ($A^{N1} = 36$, $A^{N2} = 23$ MHz)[54] and in the Met182Thr mutant ($A^{N1} = 39$, $A^{N2} = 18$ MHz).[24] Since the later two proteins lack the axial S(Met) ligation and have the two inequivalent histidines, the two high-energy transitions can reasonably be assigned to the two histidine π_1 → Cu charge-transfer transitions.

3.1.3. Comparison with Wild-Type Nitrite Reductase.
The type 1 site in nitrite reductase has the same ligand set as plastocyanin but with a shorter axial S(Met) ligand (2.55 Å in nitrite reductase vs 2.82 Å in plastocyanin). The "perturbed" type 1 copper center in the wild-type nitrite reductase exhibits dramatically different spectroscopic features (Figure 1B) compared to the classic blue copper site in plastocyanin (Table 2). The absorption intensity at 17 550 cm^{-1} (~570 nm, band 4) dramatically decreases ($\epsilon \approx 1490$ M^{-1} cm^{-1} in wild-type nitrite reductase vs $\epsilon \approx 5160$ M^{-1} cm^{-1} in plastocyanin) accompanied by a large increase in the intensity at 21 900 cm^{-1} (~450 nm, band 3, $\epsilon \approx 2590$ M^{-1} cm^{-1} in wild-type nitrite reductase vs $\epsilon \approx 600$ M^{-1} cm^{-1} in plastocyanin), leading to the green color. The higher energy band at 25 650 cm^{-1} (band 1) is due to the S(Met) → Cu charge-transfer transition and is more intense in the wild-type nitrite reductase ($\epsilon \approx 1750$ M^{-1} cm^{-1}) relative to plastocyanin ($\epsilon \approx 250$ M^{-1} cm^{-1}). Additionally, all the ligand field transitions (bands 5–8) shift to higher energy by ~1000 cm^{-1} compared to those in plastocyanin. These spectral changes have been determined to be due to (1) the rotation of the Cu $3d_{x^2-y^2}$ to σ overlap with the S(Cys) leading to the intense σ and weak π S(Cys) → Cu charge-transfer transitions and (2) tetragonal distortion leading to the increased d → d transition energies. These derive from the coupled distortion where the shorter Cu–S(Met) bond leads to longer Cu–S(Cys) bond and tetragonal rotation of the S(Met)–Cu–S(Cys) plane toward the N(His1)–Cu–N(His2) plane.

In this study, the significant spectral differences between wild-type nitrite reductase and the mutant Met182Thr have been investigated. In the charge-transfer region there is a redistribution of absorption intensities between bands 3 and 4 in Met182Thr compared to that of wild-type nitrite reductase. The S(Cys) pπ → Cu $3d_{x^2-y^2}$ transition (band 4) in Met182Thr is ~1.6 times more intense than its counterpart in the wild-type protein (2170 M^{-1} cm^{-1} in Met182Thr vs 1490 M^{-1} cm^{-1} in wild-type nitrite reductase). This is accompanied by the dramatic drop in intensity in Met182Thr for the higher energy S(Cys) pseudo-σ → Cu $3d_{x^2-y^2}$ transition (band 3, from 2590 M^{-1} cm^{-1} in wild-type nitrite reductase to 630 M^{-1} cm^{-1} in the mutant), which is the

(51) Sjölin, L.; Scholes, C. P., personal communication.
(52) Machonkin, T. E.; Quintanar, L.; Palmer, A. E.; Hassett, R.; Severance, S.; Kosman, D. J.; Solomon, E. I. *J. Am. Chem. Soc.* **2001**, *123*, 5507–5517.
(53) Randall, D. W.; George, S. D.; Hedman, B.; Hodgson, K. O.; Fujisawa, K.; Solomon, E. I. *J. Am. Chem. Soc.* **2000**, *122*, 11 620–11 631.
(54) Werst, M. M.; Davoust, C. E.; Hoffman, B. M. *J. Am. Chem. Soc.* **1991**, *113*, 1533–1538.

dominant absorption feature in nitrite reductase. Since the intensity of these transitions is proportional to the overlap of the cysteine and the Cu $3d_{x^2-y^2}$ orbitals, the increase in intensity of band 4 and the loss in intensity of band 3 in Met182Thr relative to wild-type nitrite reductase indicates that there is an increase in the S(Cys) pπ overlap and a decrease in the pseudo-σ overlap in the mutant HOMO. In addition, the higher energy bands in the Met182Thr mutant are different from those of the wild-type enzyme. In wild-type nitrite reductase the high-energy band at 25 650 cm^{-1} (band 1) is assigned to the S(Met) $\rightarrow$ Cu charge-transfer transition. Band 2, which is typically assigned to the N(His) $\rightarrow$ Cu charge-transfer transition, is not observed in wild-type nitrite reductase because of overlap with bands 1 and 3. The large absorption intensity associated with band 1 in wild-type nitrite reductase reflects the fact that significant S(Met) character is present in the HOMO and the increased intensity of band 3 is due to σ-overlap of the S(Cys) with the copper (discussed above). In the Met182Thr mutant, two bands are observed at 22 500 cm^{-1} (band 2) and 25 000 cm^{-1} (band 1'), assigned as the N(His) $\rightarrow$ Cu charge-transfer transitions (vide supra).

In the low-energy region the Gaussian fit of the absorption spectrum of Met182Thr reveals that there is a redistribution of the intensity of the ligand field absorption bands. Band 5 ($\epsilon =$ 1160 M^{-1} cm^{-1}) is more intense than band 6 ($\epsilon =$ 970 M^{-1} cm^{-1}) in wild-type nitrite reductase absorption spectrum, while band 6 ($\epsilon =$ 760 M^{-1} cm^{-1}) is relatively more intense than band 5 ($\epsilon =$ 630 M^{-1}cm^{-1}) in the Met182Thr mutant. Band 6, which is assigned as the Cu $3d_{xz+yz} \rightarrow 3d_{x^2-y^2}$ transition, gains intensity from the S(Cys) p$\pi \rightarrow$ Cu$3d_{x^2-y^2}$ transition due to configuration interaction with the S(Cys) pπ orbital.[49] Similarly, band 5, assigned as the $d_{xz-yz} \rightarrow d_{x^2-y^2}$ transition, can gain intensity due to mixing with the symmetry-allowed S(Cys) psuedo-$\sigma \rightarrow$ Cu $3d_{x^2-y^2}$ transition. The decrease in band 5 and the increase in band 6 in Met182Thr relative to wild-type nitrite reductase correlate to the decrease in the S(Cys) psuedo-$\sigma \rightarrow$ Cu $3d_{x^2-y^2}$ and increase in the S(Cys) p$\pi \rightarrow$ Cu $3d_{x^2-y^2}$ transition intensities.

The d $\rightarrow$ d transition energies in the Met182Thr mutant are very similar to those of the wild-type nitrite reductase (Table 2, bands 5$-$8). Additionally, EPR measurements have shown that the type 1 parameters ($g_z = 2.19$, $g_x = 2.02$, $g_y = 2.06$, $A_z = 67 \pm 5$ G) of the mutant are identical to the values of the wild-type enzyme.[23] The g value expressions for a singly occupied Cu $3d_{x^2-y^2}$ HOMO from ligand field theory are directly proportional to the amount of the metal d-character in the HOMO and inversely to the ligand field transition energies.[55] This would imply that the Cu d-character in the HOMO in the mutant is unchanged relative to the wild type. This suggests that the loss of the strong axial S(Met) ligand (which contributes to the HOMO) is compensated by an increase in the equatorial S(Cys)$-$Cu interaction. This increased S(Cys) covalency is observed in resonance Raman data and density functional calculations (vide infra).

3.2. Resonance Raman. Figure 2A presents the resonance Raman spectra of the Met182Thr mutant obtained with excitation at 647.1 nm into the Cu$-$S(Cys) charge-transfer band. The resonance Raman spectra of wild-type nitrite reductase using an excitation wavelength of 458 nm is presented in Figure 2B as a reference. The Met182Thr mutant spectrum displays an envelope of resonance Raman bands centered around 400 cm^{-1},
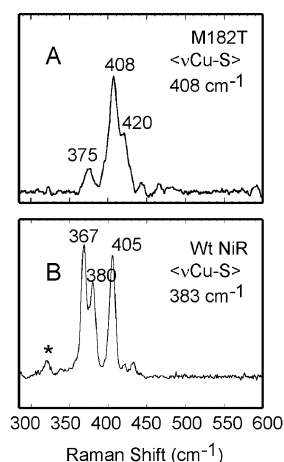
Figure 2. Resonance Raman spectra of *Rhodobacter sphaeroides* nitrite reductase Met182Thr mutant (A), excitation at 647.1 nm, and *Rhodobacter sphaeroides* nitrite reductase (B), excitation energy 458 nm.

associated with vibrations having Cu$-$S distortions. This is typically exhibited by blue copper proteins such as plastocyanin in the 350$-$500-cm^{-1} region.[56,57] The envelope is due to coupling of the Cu$-$S stretch with other modes. The envelope of bands occurs at a higher energy in Met182Thr mutant relative to that of wild-type nitrite reductase. The dominant peak is at 408 cm^{-1} in the Met182Thr mutant. There are some additional vibrations at 375 and 420 cm^{-1}. The wild-type nitrite reductase spectrum is characterized by dominant vibrations at 367, 380, and 405 cm^{-1}. (* denotes a peak from the frozen solvent).

The intensity weighted average energy of the peaks $\langle \nu_{Cu-S} \rangle$ where $\langle \nu_{Cu-S} \rangle = \Sigma_i(I_i\nu^2)/\Sigma_i(I_i\nu_i)$ has been used as an indicator of the Cu$-$S(Cys) bond strength.[56] The value of $\langle \nu_{Cu-S} \rangle$ for Met182Thr mutant is 408 cm^{-1}, and for wild-type nitrite reductase it is 383 cm^{-1}. These results indicate that the Met182Thr mutant has a stronger Cu$-$S(thiolate) bonding interaction compared to wild-type nitrite reductase. The value of $\langle \nu_{Cu-S} \rangle$ for plastocyanin is 403 cm^{-1} [56] and for fungal laccase is 419 cm^{-1}.[25] The above values suggest that the Cu$-$S(thiolate) bond strength in the Met182Thr mutant is intermediate between those of plastocyanin and fungal laccase.

3.3. Electronic Structure Calculations. In this section we consider the effect of the axial methionine ligand on the geometric and electronic structures of the blue and green Cu sites. Therefore, as starting points the blue Cu site in plastocyanin, the green Cu site in nitrite reductase, and the blue Cu site in fungal laccase (which has no axial ligand) with known experimental structures were calculated by using the B(38HF)-P86 density functional.

The experimental structures and the corresponding calculated atomic spin densities using the spectroscopically calibrated, hybrid density functional B(38HF)P86 with a theoretically converged basis set (BS5) are presented in Figure 3A$-$C. The trends in the σ/π ratios (ratio of S(Cys) 3p lobes along (σ) and perpendicular (π) to the Cu$-$S(Cys) bond) in the ground-state wave function and the covalency of the Cu$-$S(thiolate) bonds parallel the experimental results. The most covalent bond was

(55) McGarvey, B. R. In *Transition Metal Chemistry*; Carlin, B. L., Ed.; 1966; Chapter 3, pp 89$-$201.
(56) Blair, D. F.; Campbell, G. W.; Schnoover, J. R.; Chan, S. I.; Gray, H. B.; Malmström, B. G.; Pecht, I.; Swanson, B. I.; Woodruff, W. H.; Cho, W. K. *J. Am. Chem. Soc.* **1985**, *107*, 5755$-$5766.
(57) Han, J.; Adman, E. T.; Beppu, T.; Codd, R.; Freeman, H. C.; Huq, L.; Loehr, T. M.; Sanders-Loehr, J. *Biochemistry* **1991**, *30*, 10 904$-$10 913.
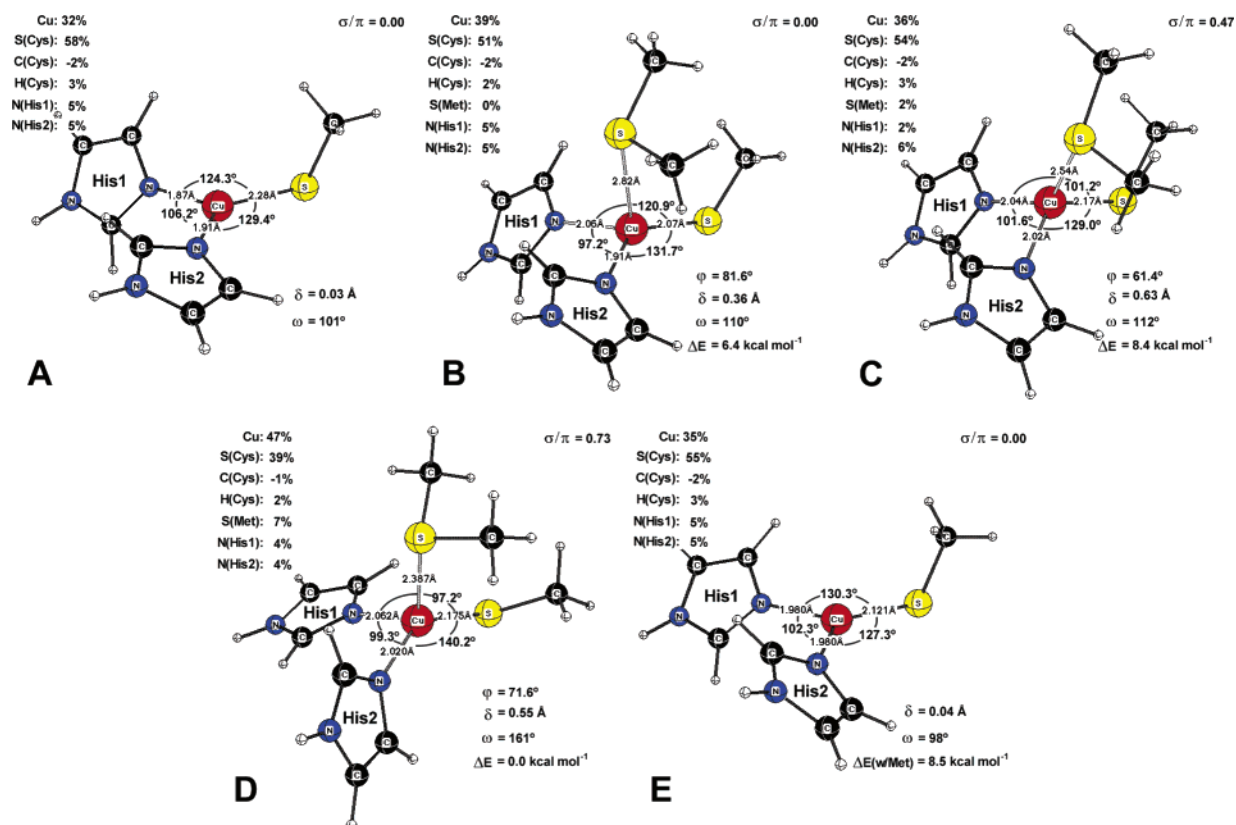
Figure 3. Experimental structures of type 1 Cu sites from fungal laccase (A), plastocyanin (B), nitrite reductase (C), and B(38HF)P86/BS5 optimized structures of computational models at strong (D) and weak (E) axial ligand limits (atomic densities from natural population analysis are given in top insets).

found in the three-coordinate, fungal laccase site (Figure 3A, calcd 58% vs exptl 55% from stellacyanin Q99L variant[58,59]), despite the long Cu−S(thiolate) bond (2.28 Å vs. 2.07 Å in blue and 2.17 Å in green sites). The Cu−S(thiolate) bond covalencies of the blue (Figure 3B, 51%) and the green (Figure 3C, 54%) sites are similar, with the latter having a slightly higher value also consistent with experiment.[18,60] Resonance Raman spectroscopy[25,56] shows that in going from the three- to four-coordinate blue site (Figure 3, A vs B), the Cu−S(thiolate) bond strength decreases ($\langle\nu\rangle_{Cu-S(Cys)}$ = 413 to 403 cm^{-1}), which parallels the change in the covalency of this bond (calcd 58% to 51%). However, in going from the four-coordinate blue to the green site, while the Cu−S(thiolate) bond strength further decreases ($\langle\nu\rangle_{Cu-S(Cys)}$ = 403 to 383 cm^{-1}, consistent with the longer bond, 2.07 to 2.17 Å), the green site is slightly more covalent (by 3%). This reflects the fact that the bonding changes from pure π (Figure 4B) to mixed σ/π character (Figure 4C) and the σ interaction has better overlap between the Cu 3d and the ligand S 3p orbitals.

The higher covalent bonding in the three-coordinate site compared with the four-coordinate sites indicates that the loss of the axial thioether interaction makes the Cu−S(thiolate) bond more covalent. The effect of the axial ligand on the geometric and electronic structures has been investigated by modeling two limits for the blue and green Cu sites: (i) the axial thioether is

present and allowed to geometry optimize and (ii) the axial thioether is eliminated and the resulting structure is optimized.

At the strong axial limit, the geometries of the green and the blue sites were optimized at the B(38HF)P86/BS5 level of theory, which gave a common equilibrium geometry (Figure 3D). This structure is rather different from what has been previously reported.[61−63] The optimized structure of the four-coordinate site has a short axial Cu−S(thioether) and a long Cu−S(thiolate) bond (2.39 and 2.19 Å, respectively). The site is tetragonally distorted and optically can be characterized as a green site due to the increased σ/π ratio (0.73 and Figure 4D) relative to both the blue (σ/π = 0.00 and Figure 4B) and the green (σ/π = 0.47 and Figure 4C) sites. In addition to the changes in the Cu−S bond length, the thiolate ligand rotates around the Cu−S bond by about 50° and the imidazole rings move within the equatorial plane to close and open the S(Cys)−Cu−N(His1) and S(Cys)−Cu−N(His2) angles by about 10° and 20°, respectively, while the N(His1)−Cu−N(His2) angle remains virtually unchanged. These changes indicate that the corresponding internal coordinates of the site are constrained by the protein environment. The magnitude of this protein effect can be estimated by back-transforming all the Cu-containing internal coordinates of the optimized site to the experimental structure, which gives energy differences of about 6−8 kcal mol^{-1}. This energy destabilization is larger than reported earlier (1−2 kcal mol^{-1}), because references 61−63 compare optimized

(58) George, S. D.; Basumallick, L.; Szilagyi, R. K.; Randall, D. W.; Hill, M. G.; Nersissian, A. M.; Valentine, J. S.; Hedman, B.; Hodgson, K. O.; Solomon, E. I. *J. Am. Chem. Soc.* **2003**, *125*, 11314−11328.
(59) The S−K edge data could not be collected for fungal laccase because of photoreduction in the beam.
(60) Shadle, S. E.; Penner-Hahn, J. E.; Schugar, H. J.; Hedman, B.; Hodgson, K. O.; Solomon, E. I. *J. Am. Chem. Soc.* **1993**, *115*, 767−776.

(61) Ryde, U.; Olsson, M. H. M.; Pierloot, K.; Roos, B. O. *J. Mol. Biol.* **1996**, *261*, 586−596.
(62) Pierloot, K.; DeKerpel, J. O. A.; Olsson, M. H. M.; Roos, B. O. *J. Am. Chem. Soc.* **1998**, *120*, 13156−13166.
(63) Kerpel, J. O. A. D.; Ryde, U. *Proteins: Struct., Funct. Genet.* **1999**, *36*, 157−174.
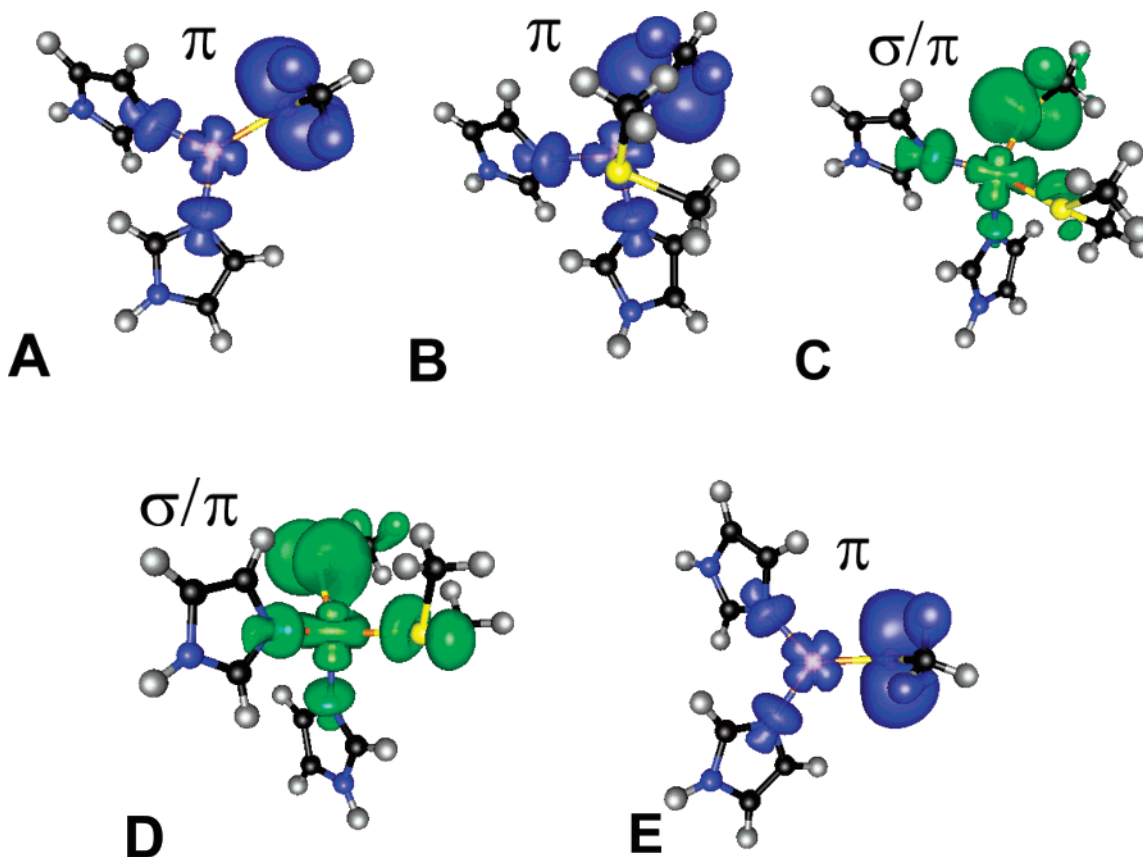
Figure 4. Spin density contour plots for the experimental structures of type 1 Cu sites from the fungal laccase (A), plastocyanin (B), nitrite reductase (C), and optimized structures of four- (D) and three-coordinate (E) computational models calculated at the B(38HF)P86/BS5 level of theory.

structures with and without constrained Cu−S(Met) bond lengths, which gives only part of the energy change associated with the protein constraint. More importantly, the energy destabilization in the oxidized structures is small compared to that of the reduced site (14−21 kcal mol^{-1}),[64] indicating the reduced site is destabilized relative to the oxidized site by the protein environment.

To consider the weak axial limit, the thioether ligand was removed from the experimental green and the blue sites and the geometry of the resulting three-coordinate site was optimized. Even for the initial, three-coordinate structures without optimization, the S atomic spin density increases by 7 and 13% and the Cu spin density decreases by 7 and 11% (not shown), respectively, relative to the blue and green experimental sites. As found for the strong axial limit, the optimizations converge to a common equilibrium geometry (Figure 3E), which is quite similar to the experimental blue Cu site in fungal laccase (Figure 3A). It is characterized by a short (2.12 Å) and highly covalent Cu−S(thiolate) bond (55% S character) and relatively short Cu−N(His) bond lengths of 1.98 Å. In comparison to the optimized four-coordinate site (Figure 3D), the equatorial bonds in the optimized three-coordinate site (Figure 3E) get shorter (Cu−S(Cys) 2.18 Å, about 2.04 Å Cu−N(His) from Figure 3D) and the electronic structure changes. The geometry-optimized four-coordinate site is green with a $\sigma/\pi = 0.73$ (Figure 4D), while the optimized three-coordinate site is blue with a $\sigma/\pi = 0.00$ (Figure 4E), consistent with the experimental spectral changes observed in this study.

(64) Solomon, E. I.; Szilagyi, R. K.; George, S. D.; Basumallick, L. *Chem. Rev.*, in press.

4. Discussion

Blue and green sites have same ligand set yet different electronic structures—while the former has S(Cys) → Cu^{II} π charge transfer (CT) the later has σ CT. This large difference in bonding has been associated with the strength of the axial S(Met) ligand−Cu^{II} bond and the associated coupled distortion. In the Met182Thr mutant the short/strong axial S(Met)−Cu^{II} bonding of the wild-type enzyme has been mutated to a threonine. There is an increase in the absorption intensity at ∼600 nm (π CT) and an accompanying decrease in intensity at ∼450 nm (σ CT), making it blue. The significance of studying this mutant is that it enables us to directly evaluate the effect of the strong axial methionine, and the properties of the blue site which result from its elimination, in the green protein matrix environment. This leads to an interesting sequence in going from plastocyanin (blue) → nitrite reductase (green) → the axial mutant of nitrite reductase (blue). This sequence is important for evaluating the protein matrix and the axial ligand contributions to the active site geometric and electronic structure.

The absorption intensity pattern in the mutant indicates an increase in the S(Cys) π−Cu interaction and a decrease in the S(Cys) pseudo σ−Cu interaction. Resonance Raman data provide direct evidence that the Cu−S(Cys) bond is stronger in the mutant relative to the wild type. Furthermore, the comparison of the ligand field transition energies of the Met182Thr mutant to other blue copper centers (plastocyanin and fungal laccase) suggests that there is a very weak axial interaction involving threonine or H$_2$O.

Interestingly, this diminished axial interaction and associated optical spectral differences in the mutant relative to the wild

type do not change some of the ground state properties (vide infra) of the mutant. The MCD assignments indicate that the ligand field transition energies have remained unchanged in the mutant compared to those in the wild type, type 1 site. This is the result of competing factors: The weaker axial S(Met), stronger equatorial S(Cys), and less tetragonal structure should shift the ligand field transitions lower in energy, while the weak axial interaction also allows the copper to shift toward the trigonal plane, which would shift the ligand field transitions in the opposite direction. EPR measurements have shown that the type 1 parameters (*g* values and copper hyperfine values) of the mutant were identical to the values in the wild type. The similar *g* values reflect the similar ligand field transition energies and imply that the Cu d character in the HOMO is similar in the wild type and the mutant. The equivalent *g* values of the mutant and the wild type further account for the lack of change in the copper hyperfine between the two proteins: the orbital dipolar coupling does not change, and the equivalent covalency leads to the same Fermi contact and the spin dipolar terms. Further, the rhombicity ($\Delta g_\perp = 0.04$) of the type 1 site remains the same in the green site (wild type) and the blue site (M182T). This is consistent with W-band EPR studies,[65] which indicate that the rhombicity of a green and a blue site could be similar.

Interestingly, the ENDOR frequencies[24] for the histidine nitrogens were unchanged in the mutant from their values in the wild-type enzyme. The dominant contribution to the hyperfine coupling (determined from the ENDOR frequencies) for a Cu−N(His) ligation is the isotropic Fermi coupling due to unpaired electron spin density on the nitrogens. The spin density on the nitrogens in the mutant and the wild type has in fact been found from density functional calculations to be equivalent.

It is particularly interesting that cysteine β methylene proton hyperfine couplings do not change though the bonding goes from π to σ. These hyperfine couplings are effected by the spin density in the S(Cys) 3p orbitals and the dihedral angle of the S−C$_\beta$–H$_\beta$ plane, with the direction of the spin containing orbital on the sulfur. In going from the crystal structure of wild-type nitrite reductase to the mutant the C$_\beta$–C(backbone) is rotated $\sim$10° about the S−C$_\beta$ bond.[51] A similar rotation is observed for the blue site of plastocyanin compared to nitrite reductase. This rotation, which effects the orientation of the cysteine β methylene protons, will oppose the effect of the change in spin density on the S(Cys) in going from σ (wild-type enzyme) to π (mutant) and would tend to limit the effect on the hyperfine coupling.

While the protein environment changes the reduction potential of a blue copper site (e.g., the structurally equivalent three coordinate blue sites in Fet3p and fungal laccases range from 430 to 800 mV), this study allows the evaluation of how the change in the electronic structure in going from the green to the blue site affects $E°$ in the same protein environment. The mutation results in the increase in reduction potential from 247 mV (wild type, green) to 350 mV (M182T, blue).[23] This indicates that the modulation of the strength of the axial ligand interaction allows the protein to tune the redox potential of the site. The extent of change is consistent with studies[66] on *Pseudomonas aeruginosa* azurin in which the naturally occurring

axial Met was mutated to a variety of other amino acids including those with noncoordinating groups such as Leu ($E°$ increased 102 mV) and the Ile ($E°$ increased 128 mV).

The spectroscopically calibrated DFT calculations reproduce the differences in electronic structure and bonding among the four-coordinate green and blue sites and three-coordinate blue (fungal laccase) sites. Calculations whose results strongly correlate with the data show that both four- and three-coordinate blue sites have pure π character, while the four-coordinate green site gains significant σ character. The DFT calculations indicate that the axial thioether ligand affects the geometric and electronic structures of the Cu site. The weak axial interaction corresponds to a trigonal geometry and a π-type Cu−S(thiolate) bond (Figure 4E). The strong axial interaction modeled by unconstrained optimization of a blue or green Cu site has a short Cu−S(thioether) bond, a tetragonally distorted geometry, and a mixed σ/π-type Cu−S(thiolate) bond (Figure 4D) as seen in the green Cu site (Figure 4C). Therefore, starting from the green site and replacing the axial thioether ligand with a very weak ligand leads to a trigonal structure, where the Cu−S(thiolate) bond gets stronger and more covalent and the site becomes optically blue due to a pure π interaction as observed experimentally for the M182T variant of nitrite reductase.

This study gives a detailed description of the electronic structure of the axial Met182Thr mutant of nitrite reductase. The data demonstrate that the mutant is very similar to a prototypical blue site as in plastocyanin. Relative to the wild-type, type 1 site in nitrite reductase, the very weak axial interaction in the mutant leads to an increase in the Cu−S(thiolate) interaction and the site being subjected to less tetragonal distortion. However, the net ligand field strength in the mutant is comparable to that of the wild type as confirmed in the MCD data, and the *g* values remain unchanged. Our experimental results are further supported by electronic structure calculations that show that the axial ligand plays a key role in determining the geometric and electronic structure of the ground state of blue, green type 1 copper sites.

Supporting Information Available: Tables of Cartesian coordinates for the density functional calculations, the electronic absorption and magnetic circular dichroism spectra of wild-type and type 2 depleted nitrite reductase, and X-band EPR spectra of the wild-type and type 2 depleted nitrite reductase and type 2 depleted form of the Met182Thr. This material is available free of charge via the Internet at http://pubs.acs.org.

JA037232T

(65) Gastel, M. v.; Boulanger, M. J.; Canters, G. W.; Huber, M.; Murphy, M. E. P.; Verbeet, M. P.; Groenen, E. J. J. *J. Phys. Chem. B* **2001**, *105*, 2236−2243.

(66) Pasher, T.; Kärlsson, B. G.; Nordling, M.; Malmström, B. G.; Vänngard, T. *Eur. J. Biochem.* **1993**, *212*, 289−296.